New Journal of Physics
The open-access journal for physics

Modulational instability and localized excitations involving two nonlinearly coupled upper-hybrid waves in plasmas

Ioannis Kourakis[1,3], **Padma Kant Shukla**[1] **and Gregor Morfill**[2]

[1] Institut für Theoretische Physik IV, Fakultät für Physik und Astronomie, Ruhr-Universität Bochum, D-44780 Bochum, Germany

[2] Max-Planck Institut für extraterrestrische Physik, Giessenbachstrasse, D-85740 Garching, Germany

E-mail: ioannis@tp4.rub.de, ps@tp4.rub.de and gem@mpe.mpg.de

New Journal of Physics **7** (2005) 153
Received 6 May 2005
Published 30 June 2005
Online at http://www.njp.org/
doi:10.1088/1367-2630/7/1/153

Abstract. The nonlinear coupling between two perpendicularly propagating (with respect to the external magnetic field direction) upper-hybrid (UH) waves in a uniform magnetoplasma is considered, taking into account quasi-stationary density perturbations which are driven by the UH wave ponderomotive force. This interaction is governed by a pair of coupled nonlinear Schrödinger equations (CNLSEs) for the UH wave envelopes. The CNLSEs are used to investigate the occurrence of modulational instability. Waves in the vicinity of the UH resonance are considered, so that the group dispersion terms for both waves are approximately equal, but the UH wave group velocities may be different. It is found that a pair of unstable UH waves (obeying anomalous group dispersion) yields an increased instability growth rate, while a pair of stable UH waves (individually obeying normal group dispersion) remains stable for equal group velocities, although it is destabilized by a finite group velocity mismatch. Stationary nonlinear solutions of the CNLSEs are presented.

[3] Author to whom any correspondence should be addressed.

PII: S1367-2630(05)99543-8

Contents

1. Introduction

High-frequency upper-hybrid (UH) plasma waves [1, 2] have attracted particular interest among plasma researchers, due to their occurrence in space and laboratory plasmas. The Whisper and Peace instruments on board the Cluster space mission [3] provide abundant evidence for the occurrence of UH wave-related phenomena in the magnetosphere. Back to Earth-based applications, the availability of high-power microwave sources has enabled the implementation of efficient plasma heating scenario in tokamak fusion reactors [4, 5]; electron–cyclotron heating, UH mode conversion and related parametric instabilities are among the effective heating mechanisms so far suggested [6]–[8].

Increased attention has been drawn to nonlinear phenomena, such as localized modes (e.g. soliton excitations), instabilities and ponderomotive coupling effects related to plasma modes, in the last few decades. Super Alfvénic UH solitons were discovered by Kaufman and Stenflo [9]. Porkolab and Goldman [10] presented a detailed investigation of the UH envelope soliton formation. Yu and Shukla [11] pointed out the existence of cusped UH envelope solitons on the timescale of an ion cyclotron (gyro-)period. Subsequent studies then focused on the oblique propagation of large amplitude nonlinear waves (also elucidating the role of the electric field) [12], decay interactions and envelope modulation [13]–[16], and ponderomotive coupling effects [12], [17]–[19], modelling soliton formation via generic Korteweg–de Vries (KdV) and modified KdV [12, 16], as well as nonlinear Schrödinger (NLS) equation [10]–[18] related formalisms.

From a wider point of view, the study of the amplitude modulation of nonlinear waves propagating in dispersive media [20, 21], known to be related to phenomena such as the modulational instability, harmonic generation and energy localization via localized structure formation, generically relies on NLS type equations [22]. A set of coupled equations of this kind naturally occurs when interactions among more than one wave is considered; the structure of these equations (not necessarily unified, and in fact often asymmetric) depends on the physical aspects of each particular problem considered. Coupled NLS equations, such as the ones derived and analysed here, occur in a variety of self-focusing, self-trapping and localization related

phenomena, in physical contexts as diverse as electromagnetic wave propagation in nonlinear media [23, 24], optical fibres [25, 26], Langmuir plasma waves [27, 28], transmission lines [29], and more recently Bose–Einstein condensates [30] and left-handed metamaterials [31, 32]. Our results are qualitatively reminiscent of those studies.

In this paper, we are interested in studying the parametric coupling between two large-amplitude UH waves, propagating across the magnetic field, and ponderomotively driven quasi-stationary density perturbations. The outline of the paper goes as follows. A pair of coupled cubic time-dependent nonlinear Schrödinger equations (CNLSEs) are obtained, in section 2, describing the spatio-temporal evolution of the modulated UH electric field envelopes. The modulational stability of a single UH wave (uncoupled wave limit) is briefly analysed in section 3. The CNLSEs are used to investigate the modulational instability of the coupled UH waves in section 4. The formation of single and coupled bright and dark/grey envelope soliton excitations is reviewed in section 5, where explicit coupled soliton profiles are presented. The results are then summarized in the concluding section 6.

2. The model

We are interested in studying the propagation of nonlinearly coupled UH waves in a fully ionized, uniform collisionless plasma consisting of the electrons (mass m_e, charge $q_e = -e$; e denotes the absolute value of the electron charge) and ions (denoted by 'i'; mass m_i, charge $q_i = +e$), embedded in an external magnetic field $\mathbf{B} = B_0\hat{\mathbf{z}}$, where B_0 is the strength of the magnetic field and $\hat{\mathbf{z}}$ is the unit vector along the $z-$axis. $n_{i/e,0}$ denotes the ion/electron number density at equilibrium, where overall charge neutrality is assumed. Transverse propagation is assumed throughout this paper, i.e. $\mathbf{k}\cdot\mathbf{B} = 0$. To be specific, we consider the nonlinear coupling between two UH waves, which are associated with an electric field $\mathbf{E}_j$ (the index $j = 1, 2$ distinguishes the two UH waves, but may be omitted whenever obvious), and quasi-stationary density perturbations modulating the UH waves.

In a uniform magnetoplasma, the (transverse) UH wave frequency ω and the wavenumber $\mathbf{k}$ are related by the dispersion relation [15]

$$\omega^2 = \omega_{UH}^2 + \frac{3v_{th,e}^2k^2\omega_{p,e}^2}{\omega_{p,e}^2 - 3\omega_{c,e}^2}, \tag{1}$$

where $\omega_{UH} = (\omega_{p,e}^2 + \omega_{c,e}^2)^{1/2}$ is the UH resonance frequency, $\omega_{p,e} = (4\pi ne^2/m_e)^{1/2}$ is the electron plasma frequency, $\omega_{c,e} = eB_0/m_ec$ is the electron cyclotron (gyro-) frequency, and $v_{th,e} = (T_e/m_e)^{1/2}$ is the electron thermal speed. We see that the dispersion characteristics essentially depend on the ratio

$$\alpha \equiv \frac{\omega_{c,e}^2}{\omega_{p,e}^2} = \frac{B_0^2}{4\pi nm_ec^2},$$

as $\omega^2/\omega_{p,e}^2 = 1 + \alpha + 3k^2\lambda_{D,e}^2/(1 - 3\alpha)$, where we have defined the electron Debye length $\lambda_{D,e} = \omega_{p,e}/v_{th,e}$. In the limit of a vanishing magnetic field, one recovers from equation (1) the familiar dispersion relation for electron plasma waves in a dense plasma.

The interaction between UH waves and quasi-stationary density perturbations produces an electric field envelope of the UH waves, in the form $\tilde{E}(z, t) = (1/2)E(z, t)\exp[\mathrm{i}(kx - \omega t)] + \mathrm{cc}$

(complex conjugate). According to the standard formalism, the slowly varying field envelope $E(z, t)$ obeys an NLS-type equation; in our case, one obtains a pair of (coupled) equations of the form

$$\mathrm{i}\left(\frac{\partial E_j}{\partial t} + v_{g,j}\frac{\partial E_j}{\partial z}\right) + P_j\frac{\partial^2 E_j}{\partial z^2} - \Delta\omega_j E_j = 0 \tag{2}$$

($j = 1, 2$) [33, 34]. Here,

$$v_{g,j} = \omega_j'(k_j) = \frac{3v_{th,e}^2 k_j}{\omega_j(1 - 3\omega_{c,e}^2/\omega_{p,e}^2)} \tag{3}$$

is the group velocity of long-wavelength UH waves. The group velocity dispersion (GVD) coefficients (related to the curvature of the dispersion curve) read

$$P_j = \frac{\omega_{g,j}''(k_j)}{2} = \frac{3\omega_{UH}^2 v_{th,e}^2}{2\omega[\omega_{UH}^2(1 - 3\omega_{c,e}^2/\omega_{p,e}^2) + 3v_{th,e}^2 k_j^2]}. \tag{4}$$

Near the UH resonance frequency, i.e. for $k \ll \omega_{p,e}/v_{th,e} \equiv \lambda_{D,e}^{-1}$, the latter relations reduce to

$$v_{g,j} \approx \frac{3v_{th,e}^2 k_j}{\omega_{UH}(1 - 3\omega_{c,e}^2/\omega_{p,e}^2)} \equiv v_{j,0} \tag{5}$$

and

$$P_j \approx \frac{3v_{th,e}^2}{2\omega_{UH}(1 - 3\omega_{c,e}^2/\omega_{p,e}^2)} \equiv P_0. \tag{6}$$

It is interesting to point out that an inverse parabolic dispersion curve (with positive curvature $\omega_j''(k) > 0$) is obtained for $\omega_{c,e} > \omega_{p,e}/\sqrt{3}$, for both UH waves ($j = 1, 2$). In other words, UH waves are characterized by anomalous (normal) group dispersion, i.e. $P_j > 0$ ($P_j < 0$), if $\omega_{c,e}/\omega_{p,e} < 1/\sqrt{3}$ ($\omega_{c,e}/\omega_{p,e} > 1/\sqrt{3}$, respectively) (This criterion is valid for both relations (4), for low k_j, and (6).) Interestingly, two long-wavelength UH waves may possess different group velocities, but approximately identical curvature, i.e. $P_1 \approx P_2 \approx P_0$. The behaviour of the quantities defined here is depicted in figures 1 and 2.

The nonlinear frequency shift $\Delta\omega_j$ is given by

$$\Delta\omega_j \approx \frac{\omega_{p,e}^2}{2\omega_{UH}}N, \tag{7}$$

where the streaming electron fluid velocity associated with the plasma slow motion is assumed to be much smaller than the group velocity of the UH waves. Here $N = \delta n_e/n_0$ denotes the ratio between the electron density perturbation δn_e, associated with quasi-stationary slow plasma motion, and the equilibrium plasma number density n_0 (recall that $n_{e,0} \approx n_{i,0} \equiv n_0$, since we assume overall quasi-neutrality near equilibrium).

The quasi-stationary plasma slow motion is governed by the inertialess electron and ion momentum equations, including the UH wave ponderomotive force which basically acts on the

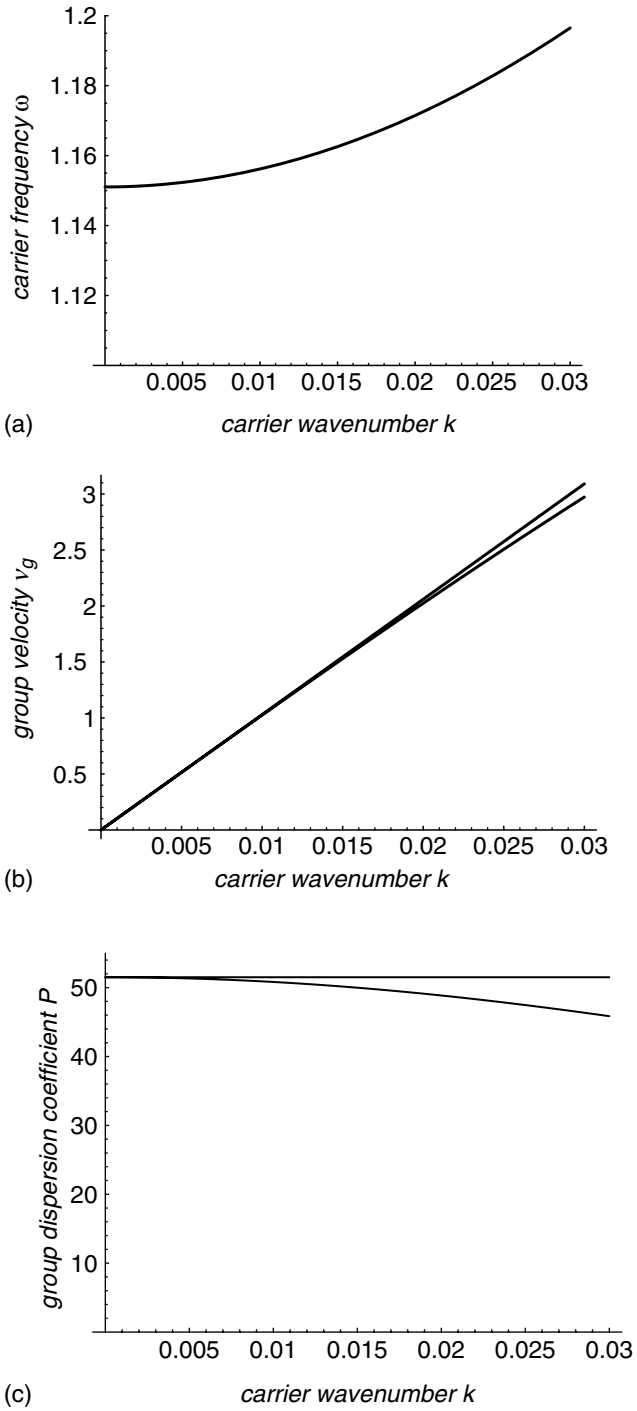

Figure 1. The dispersion laws for the UH waves: (a) the wave frequency $\omega(k)$ (scaled by ω_{pe}); (b) the group velocity $v_g = \omega'(k)$ (scaled by $v_{th,e}$) and (c) the group dispersion coefficient $P = \omega''(k)/2$ (scaled by $v_{th,e}^2/\omega_{pe}$), are depicted against the wavenumber k (scaled by $k_D = \lambda_{D,e}^{-1}$). The lower and upper curves in (b) and (c) respectively, correspond to the exact and approximate expressions, given (by (3) and (5) (by (4) and (6) respectively). Here, we have taken $\omega_{c,e}/\omega_{p,e} = 0.57$, i.e. right below the threshold $1/\sqrt{3} \approx 0.577$.

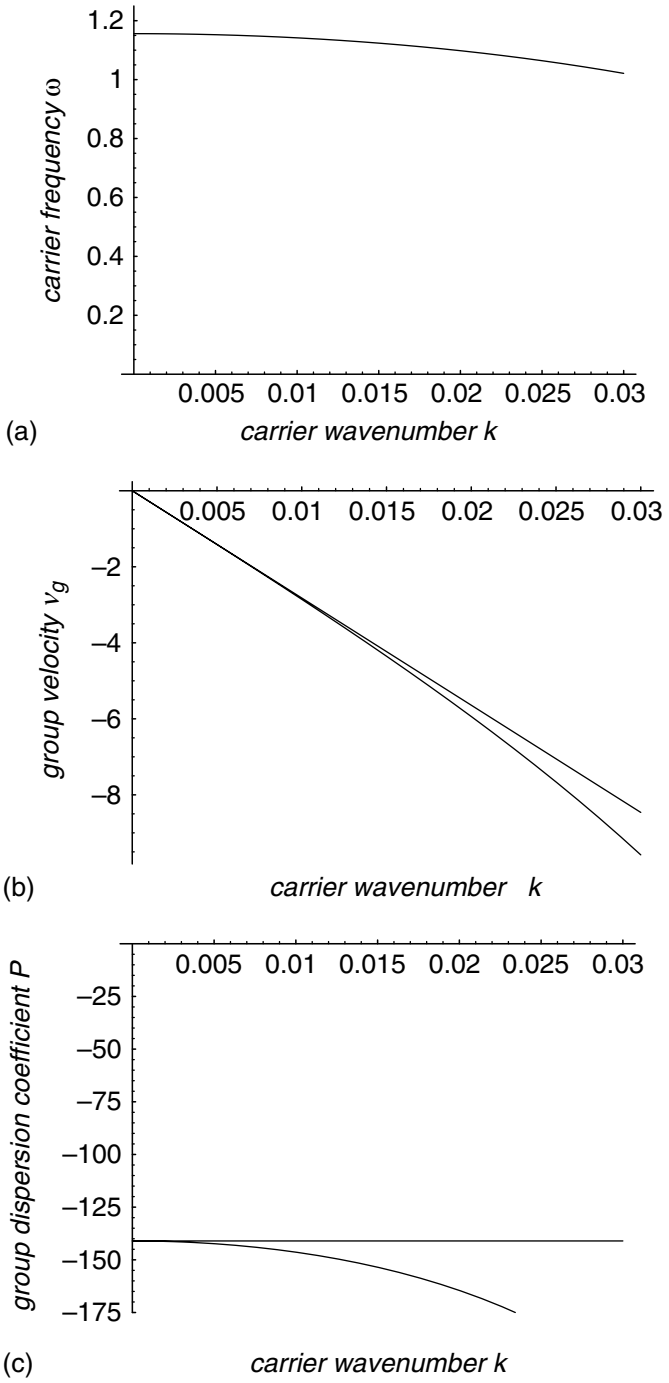

Figure 2. The dispersion laws for the UH waves: (a) the wave frequency $\omega(k)$ (scaled by ω_{pe}); (b) the group velocity $v_g = \omega'(k)$ (scaled by $v_{th,e}$) and (c) the group dispersion coefficient $P = \omega''(k)/2$ (scaled by $v_{th,e}^2/\omega_{pe}$), are depicted against the wavenumber k (scaled by $k_D = \lambda_{D,e}^{-1}$). The lower and upper curves in (b) and (c), respectively correspond to the exact and approximate expressions, given by (3) and (5) (by (4) and (6) respectively). Here, we have taken $\omega_{c,e}/\omega_{p,e} = 0.58$, i.e. right above the threshold $1/\sqrt{3} \approx 0.577$. Notice the inverse parabolic dispersive character of the UH in this parameter range (cf figure 1).

electrons. Adding the parallel component of the electron and ion momentum equations, we then obtain for our purposes

$$N \approx -\sum_{l=1}^{2} \frac{1}{4\pi n_0 T}(|E_l|^2 - |E_{l,\infty}|^2), \tag{8}$$

where $T = T_e + T_i$ (here $T_{e/i}$ denotes the electron/ion temperature; the specific heat ratios $\gamma_{e/i}$ are taken equal to unity, for adiabatic plasma compression). The integration constant $E_{l,\infty}$ essentially denotes the value of the electric field at infinity. The lengthy details of the derivation of equation (8), here omitted for simplicity, are identical to those reported in [11, 12]. The (three) evolution equations (2) and (8) now form a closed system, which describes the simultaneous evolution of the relative plasma density perturbation N and the electric field amplitude E. One notices in the right-hand side of (8) the appearance of the UH ponderomotive force ($\sim|E|^2$) acting on the electrons involved in the plasma slow motion. Combining the above expression with (7) we obtain

$$\Delta\omega_j = -\frac{\omega_{p,e}^2}{2\omega_{UH}} \sum_{l=1}^{2} \frac{1}{4\pi n_0 T}(|E_l|^2 - |E_{l,\infty}|^2) \equiv -\sum_{l=1}^{2} Q_{jl}(|\mathcal{E}_l|^2 - |\mathcal{E}_{l,\infty}|^2), \tag{9}$$

where $\mathcal{E}_l = E_l/\sqrt{4\pi n_0 T}$. The definition of the (four equal) quantities $Q_{jl} = Q$ (for $j, l = 1, 2$) is obvious, upon inspection, i.e. $Q = \omega_{p,e}^2/2\omega_{UH}$; we notice that Q is a positive real quantity.

The set of equations (2) can now be cast in the form of CNLSEs

$$\begin{aligned} &\mathrm{i}\left(\frac{\partial \mathcal{E}_1}{\partial t} + v_{g,1}\frac{\partial \mathcal{E}_1}{\partial z}\right) + P_1\frac{\partial^2 \mathcal{E}_1}{\partial z^2} + Q_{11}|\mathcal{E}_1|^2\mathcal{E}_1 + Q_{12}|\mathcal{E}_2|^2\mathcal{E}_1 = 0, \\ &\mathrm{i}\left(\frac{\partial \mathcal{E}_2}{\partial t} + v_{g,2}\frac{\partial \mathcal{E}_2}{\partial z}\right) + P_2\frac{\partial^2 \mathcal{E}_2}{\partial z^2} + Q_{22}|\mathcal{E}_2|^2\mathcal{E}_2 + Q_{21}|\mathcal{E}_1|^2\mathcal{E}_2 = 0. \end{aligned} \tag{10}$$

Despite the apparent symmetry in the nonlinear part of these equations (recall that $Q_{ij} = Q$ here), we have chosen to keep the subscript notation below, for the sake of analytical comparison with different physical contexts, where CNLSEs formally identical to equations (10) arise. Recall that P_j and $v_{g,j}$ are positive (negative) if the ratio α is below (above) 1/3.

In the following, we shall first briefly recall part of the existing knowledge on a single UH wave (uncoupled wave limit), and then proceed by examining the modulational (in)stability of coupled UH waves. We shall show that the stability profile is essentially related to the sign of the GVD coefficient P_j, and investigate the effect of the interaction on UH wave stability.

3. Modulational (in)stability of single UH waves

It is instructive to review the stability analysis and relevant results obtained for the uncoupled single UH wave case [10], which is obtained by 'switching off' the coupling, i.e. by formally setting $E_{j'}$ ($j' \neq j$, any of 1 and 2) to zero in equations (10). The well known (single) NLS equation for the jth field amplitude is thus obtained (the index $j = 1$ or 2 will be omitted where obvious). Making use of the generic NLS formalism, presented in detail elsewhere (see e.g. in

[20]–[22]), one expects the electric field envelope $\mathcal{E}_j$ (in the absence of its counterpart E'_j) to be 'modulationally unstable' if $P_j Q_{jj}$ (or, simply, P_j here) is positive, i.e. if $\sqrt{\alpha} < 1/\sqrt{3}$. To see this, one may first check that the (single, now) NLS equation obtained from (10) is satisfied by the plane wave solution $\mathcal{E}_j(z,t) = \mathcal{E}_0 \mathrm{e}^{\mathrm{i}Q_{jj}|\mathcal{E}_0|^2 t} + \mathrm{cc}$. The standard (linear) stability analysis then shows that a linear modulation with frequency Ω and wavenumber K obeys the dispersion relation

$$(\Omega - v_{g,j}K)^2 = P_j K^2 (P_j K^2 - 2Q_{jj}|\mathcal{E}_0|^2), \tag{11}$$

which exhibits an oscillatory instability if $K \leqslant K_{cr,0} = (2Q_{jj}/P_j)^{1/2}|\mathcal{E}_0|$. The growth rate $\sigma = \mathrm{Im}(\Omega)$ attains a maximum value $\sigma_{max} = Q_{jj}|\mathcal{E}_0|^2$. For $P_j < 0$, on the other hand, i.e. if $\sqrt{\alpha} > 1/\sqrt{3}$, the wave is modulationally stable, as evident from (11).

We notice that the characteristic quantity $|Q_{jj}/P_j|^{1/2}$ (bearing dimensions of an inverse length), which determines the critical wavenumber $K_{cr,0}$ above and the soliton characteristics (as we shall see below), here essentially depends on the plasma parameters as $|Q_{jj}/P_j|^{1/2} \sim (1/3 - \omega_{c,e}^2/\omega_{p,e}^2)^{1/2}\, \omega_{p,e}/v_{th,e} = |1/3 - \alpha|^{1/2}/\lambda_{D,e}$.

Summarizing, for a ratio α below (above) $1/3$, where P is positive (negative), an UH wave is unstable (stable) against quasi-stationary density perturbations that are self-consistently excited by the UH wave ponderomotive force.

4. Coupled UH waves: stability analysis

Let us now consider the complete pair of electric field envelope functions $\mathcal{E}_{1/2}$, whose evolution obeys the coupled NLS equations (10) above. In order to investigate the coupled UH wave stability, we shall first seek an equilibrium state by inserting the ansatz $\mathcal{E}_j = \mathcal{E}_{j0} \exp[\mathrm{i}\varphi_j(t)]$, where $\mathcal{E}_{j0}$ is a (constant real) amplitude and $\varphi_j(t)$ is a (real) phase, into equations (10). We thus find a monochromatic (fixed-frequency) solution of the form $\varphi_j(t) = \Omega_{j0}t$, where

$$\Omega_{j0} = Q_{jj}\mathcal{E}_{j0}^2 + Q_{jl}\mathcal{E}_{l0}^2 = Q(\mathcal{E}_{10}^2 + \mathcal{E}_{20}^2),$$

for $j, l = 1, 2$ $(l \neq j)$.

Let us consider a small perturbation around the stationary state defined above by taking $\mathcal{E}_j = (\mathcal{E}_{j0} + \epsilon\mathcal{E}_{j1}) \exp[\mathrm{i}\varphi_j(t)]$, where $\epsilon\mathcal{E}_{j1}(\mathbf{r}, t)$ is a small ($\epsilon \ll 1$) amplitude perturbation of the slowly varying modulated field amplitudes, and $\varphi_j(t)$ is the phasor defined above. Substituting into equations (10) and separating the real and imaginary parts by writing $\mathcal{E}_{j1} = a_j + \mathrm{i}b_j$ $(a_j, b_j \in \Re)$, the first-order terms (in ϵ) yield

$$-\frac{\partial b_j}{\partial t} - v_{g,j}\frac{\partial b_j}{\partial z} + P_j\frac{\partial^2 a_j}{\partial z^2} + 2Q_{jj}\mathcal{E}_{10}^2 a_j + 2Q_{jl}\mathcal{E}_{j0}\mathcal{E}_{l0}a_l = 0, \qquad \frac{\partial a_j}{\partial t} + v_{g,j}\frac{\partial a_j}{\partial z} + P_j\frac{\partial^2 b_j}{\partial z^2} = 0, \tag{12}$$

where j and l $(\neq j) = 1, 2$ (this will henceforth be understood unless otherwise stated). Eliminating b_j, these equations yield

$$\left[\left(\frac{\partial}{\partial t} + v_{g,j}\frac{\partial}{\partial z}\right)^2 + P_1\left(P_1\frac{\partial^2}{\partial z^2} + 2Q_{11}\mathcal{E}_{10}^2\right)\frac{\partial^2}{\partial z^2}\right]a_1 + 2P_1Q_{12}|\mathcal{E}_{10}||\mathcal{E}_{20}|\frac{\partial^2}{\partial z^2}a_2 = 0, \tag{13}$$

(along with a symmetric equation, obtained by permuting $1 \leftrightarrow 2$). We now let $a_j = a_{j0} \exp[\mathrm{i}(Kz - \Omega t)] + \mathrm{cc}$, where K and Ω_k are the wavevector and the frequency of the modulation, respectively, i.e. $\partial/\partial t \to -\mathrm{i}\Omega$ and $\partial/\partial z \to \mathrm{i}K$, i.e. $\partial^2/\partial t^2 \to -\Omega^2$ and $\partial^2/\partial z^2 \to -K^2$. After some straightforward algebra, we obtain a nonlinear dispersion relation of the form

$$[(\Omega - v_{g,1}K)^2 - \Omega_1^2][(\Omega - v_{g,2}K)^2 - \Omega_2^2] - \Omega_c^4 = 0, \tag{14}$$

where we have defined the quantities as $\Omega_j^2 \equiv P_j K^2 (P_j K^2 - 2Q_{jj}|\mathcal{E}_{j0}|^2)$ (for $j = 1, 2$), and $\Omega_c^4 \equiv 4P_1P_2Q_{12}Q_{21}|\mathcal{E}_{10}|^2|\mathcal{E}_{20}|^2K^4 = 4P_1P_2Q^2|\mathcal{E}_{10}|^2|\mathcal{E}_{20}|^2K^4$. The relation (14) is essentially a fourth-order polynomial equation in Ω.

4.1. Equal group velocities

For the sake of analytical tractability, one may assume that the two UH waves are characterized by equal group velocities $v_{g,1} = v_{g,2}$, since one is interested in the dynamics near the UH resonance (for $k \approx 0$, so $P_1 = P_2 = P$ as well). Thus, setting $v_{g,j} \approx 0$, we obtain the eigenvalue problem: $\mathbf{Ma} = \omega^2\mathbf{a}$, where $\mathbf{a} = (a_1, a_2)^T$ is the vector of the (real part of) perturbation amplitudes, and the matrix elements are given by $M_{jj} = \Omega_j^2$ and $M_{jl} = -2P_jQ_{jl}|\mathcal{E}_{j0}||\mathcal{E}_{l0}|K^2$ (for $l \neq j$, both equal to 1 or 2), thus $M_{12}M_{21} = \Omega_c^4$. We note that M_{11} and M_{22} bear the same functional form, in terms of K and $|\mathcal{E}_{10}|$ or $|\mathcal{E}_{20}|$, respectively, for $P_1 \approx P_2$ and $Q_{jl} = Q > 0$ ($\forall j, l = 1, 2$); also, $M_{12} = M_{21}$ here.

The perturbation frequency Ω and wavenumber K are related by the reduced nonlinear dispersion relation

$$(\Omega^2 - \Omega_1^2)(\Omega^2 - \Omega_2^2) = \Omega_c^4, \tag{15}$$

where the coupling is expressed via $\Omega_c^4 = M_{12}M_{21}$ in the right-hand side of equation (15). The nonlinear dispersion relation (15) takes the form of a bi-quadratic polynomial equation

$$\Omega^4 - T\Omega^2 + D = 0, \tag{16}$$

where $T = \mathrm{Tr}\,\mathbf{M} \equiv \Omega_1^2 + \Omega_2^2 = 2P^2K^2[K^2 - (Q/P)\sum_j |\mathcal{E}_{j0}|^2]$ and $D = \mathrm{Det}\,\mathbf{M} \equiv \Omega_1^2\Omega_2^2 - \Omega_c^4 = P^4K^6[K^2 - 2(Q/P)\sum_j |\mathcal{E}_{j0}|^2]$ are the trace and the determinant, respectively, of the matrix $\mathbf{M}$. Equation (16) admits the solution

$$\Omega^2 = \tfrac{1}{2}[T \pm (T^2 - 4D)^{1/2}]. \tag{17}$$

We note that the right-hand side is real in our case, since the discriminant quantity $\Delta = T^2 - 4D = (\Omega_1^2 - \Omega_2^2)^2 + 4\Omega_c^4$ is a positive quantity here, as one may readily check.

Stability is ensured (for any wavenumber K) if (and only if) both solutions $\Omega_\pm^2$ are positive real numbers. Recalling that the sum and the product of the (real, since $\Delta > 0$) roots of the polynomial $p(x) = x^2 - Tx + D$ are given by T and D, respectively, the stability requirement is tantamount to the following conditions being satisfied simultaneously: $T > 0$ and $D > 0$. It is easy to check that,

(i) if $P < 0$ (hence if each UH wave is individually stable; see above), the UH wave pair will be stable (for every value of K and $\mathcal{E}_{j,0}$); on the other hand,

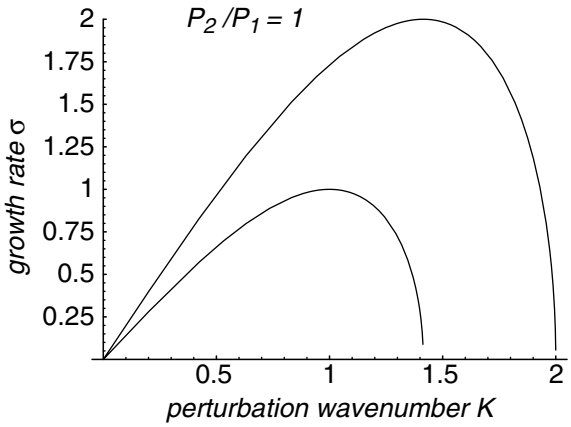

Figure 3. (Unstable–unstable UH wave coupling) The instability growth rate σ_1 of a single unstable wave 1—e.g. $\sigma_1 = -\Omega_1^2$ (lower curve) and that of an unstable–unstable UH wave pair (i.e. $\sigma_1^2 = -\Omega_-^2 > 0$, for $P_1 = P_2 = P > 0$; upper curve) are depicted against the perturbation wavenumber K (normalized by $\sigma_0 = Q|\mathcal{E}_{1,0}|^2$ and $K_{cr,0} = (2Q/P)^{1/2}\,|\mathcal{E}_{1,0}|$, respectively), for $|\mathcal{E}_{1,0}| = |\mathcal{E}_{2,0}|$, $P_2 = P_1 = 1$ and $Q_{ij} = 1$ (i, $j = 1, 2$).

(ii) if $P > 0$, (i.e. if each UH wave is individually unstable; see above), then the UH wave pair will be unstable to external perturbations with a wavenumber $K < [2(Q/P)\sum_j |\mathcal{E}_{j0}|^2]^{1/2} \equiv K_{cr}$ (i.e. $D < 0$, so $\Omega_-^2 < 0$). In simple terms, for any given (finite) perturbation wavenumber K, it suffices to consider a pair of perturbation amplitudes satisfying $|\mathcal{E}_{10}|^2 + |\mathcal{E}_{20}|^2 > PK^2/(2Q)$, or $|\mathcal{E}_{20}|^2/|\mathcal{E}_{10}|^2 > K^2/K_{cr,0}^2 - 1$ (cf the definition of $k_{cr,0}$ in section 3; we see that not only is this relation always satisfied if $K \leqslant K_{cr,0}$, but it may also satisfied for higher K, implying a wider unstable wavenumber range). Specifically, for $K_{cr}/\sqrt{2} < K < K_{cr}$ (i.e. $D < 0 < T$), one has $\Omega_-^2 < 0 < \Omega_+^2$, while for $0 < K < K_{cr}/\sqrt{2}$ (i.e. $T < 0 < D$), one has $\Omega_-^2 < \Omega_+^2 < 0$. The growth rate σ of the instability in both cases will be determined as $\sigma = \mathrm{i}\sqrt{-\Omega_-^2}$, and will be increased, compared to the single UH wave growth rate $Q|E_j|^2$ (see above), as one may readily check, either analytically or numerically; see figure 3.

4.2. Different group velocities

Let us now consider two UH waves which are characterized by $P_1 \approx P_2 = P$, but $v_{g,1} \neq v_{g,2}$; this is true for very large (but finite) UH wavelengths. The dispersion relation (14) now determines a fourth order polynomial equation in Ω (although, in fact, 16th order in K), say $p(\Omega, K) = 0$, whose solutions (and associated existence criteria) need to be investigated. The expanded form of $p(\Omega, K)$ is readily obtained from equation (14) (together with the associated definitions) and need not be exposed here. Let us just point out that the cubic and linear terms in the frequency (i.e. $\sim\Omega^3$, Ω^1) are preceded by coefficients which cancel for vanishing group velocities, thus resulting in a bi-quadratic polynomial (with terms $\sim\Omega^4$, Ω^2, Ω^0), as we saw above. In view of obtaining the exact solution for Ω in terms of K (for a given set of parameter values for P, Q, $\mathcal{E}_{10}$, $\mathcal{E}_{20}$), one may either employ the existing (complicated) analytical formulae (and associated criteria) for the solutions of a fourth order polynomial, which can be found in mathematical formularies,

or engage in a detailed numerical investigation. We have chosen to do neither here. Instead, we shall see that despite the apparent complexity of this task, some interesting qualitative results can be obtained from the dispersion relation (14) on the role of the group velocity mismatch, by efficiently employing very simple arguments.

Inspired by an idea proposed in [27], we may express the general dispersion relation (14) in the form

$$f_1(x) = f_2(x), \tag{18}$$

where we have defined the functions

$$f_1(x) = (x - x_1)^2 + A, \qquad f_2(x) = \frac{C}{(x - x_2)^2 + B}, \tag{19}$$

and the real quantities $x_j = K v_{g,j}$, $A = -\Omega_1^2 = -M_{11}$, $B = -\Omega_2^2 = -M_{22}$ and $C = \Omega_c^4 = M_{12}M_{21}$ (here $C > 0$, since $M_{12}M_{21} \sim P_1 P_2 Q_{12} Q_{21} = P^2 Q^2 > 0$; cf the definitions above); the variable x here denotes Ω. Equation (18) possesses four complex solutions, each of which may (or may not) be real (i.e. possess a vanishing imaginary part). Now, the stability profile of a coupled UH wave pair is determined by the number of real solutions of equation (18), which is an integer, say r, between 0 and 4. For absolute stability (for any K, $|\mathcal{E}_{j0}|$), we need to have four real solutions; in any other case, i.e. if $r < 4$, the remaining $4 - r$ complex solutions determine (via their imaginary part) the growth rate of the instability which may develop. Note that (the relative magnitude of) x_1 and x_2 express the group velocity mismatch ($v_{g,1} = v_{g,2}$ for $x_1 \neq x_2$).

Let us study the functions $f_1(x)$ and $f_2(x)$. The former one is a parabola, which possesses a minimum at (x_1, A). The latter one is characterized by a local maximum (since $C > 0$) at $(x_2, C/B)$, in addition to a horizontal asymptote (the x-axis), since $f_2(x) \to 0$ for $x \to \pm\infty$. Furthermore, for $B < 0$ (only), $f_2(x)$ has two vertical asymptotes (poles) at $x = x_2 \pm \sqrt{|B|}$ (see figures 4 and 5). Now, two combinations of parameter values need to be distinguished, namely: (i) the case of a stable–stable (individually) UH wave pair ($P_1 < 0$ and $P_2 < 0$), and (ii) an unstable–unstable (individually) UH wave pair ($P_1 > 0$ and $P_2 > 0$).

Firstly, for a stable–stable UH wave pair (i.e. for $P_1 < 0$ and $P_2 < 0$), we have seen that the reduced dispersion relation (15) predicted stability. This result regarded the equal group velocity case, $v_{g,1} = v_{g,2}$, and may be visualized by plotting $f_1(x)$ and $f_2(x)$ for $x_1 = x_2$ and $A, B < 0$ (since $P_1, P_2 < 0$); see figure 4(a). We stress the fact that $D = M_{11}M_{22} - M_{12}M_{21} = AB - C$ turns out to be positive here, implying (for $B < 0$) that $A < C/B$; thus, the minimum of $f_1(x)$ lies always below the local maximum of $f_2(x)$. Thus, four points of intersection always exist (cf figure 4(a)), for $x_1 = x_2$ and $A, B < 0$; this fact ensures stability, as we saw, for $v_{g,1} = v_{g,2}$ and $M_{11}, M_{22} > 0$ (both UH waves individually stable). Now, considering $v_{g,1} \neq v_{g,2}$ results in a horizontal shift between the two curves (cf figure 4(b)), which may exactly result in reducing the number of intersection points from 4 to 2 (enabling instability). Therefore, a pair of stable UH waves may be destabilized due to a finite difference in group velocity, i.e. $v_{g,2} - v_{g,1} \neq 0$.

Let us now consider an unstable–unstable UH wave pair (i.e. for $P_1 > 0$ and $P_2 > 0$). We have previously seen that the reduced dispersion relation (15) predicted instability in this case. One might naturally wonder whether this result, which regarded the equal group velocity case ($v_{g,1} = v_{g,2}$), still holds its validity for different $v_{g,j}$. Pretty much as we did above, this result (for $v_{g,1} = v_{g,2}$) may be visualized by plotting $f_1(x)$ and $f_2(x)$ for $x_1 = x_2$ and $A, B > 0$ (since $P_1, P_2 > 0$); see figure 5(a). Here, the fact that $D = M_{11}M_{22} - M_{12}M_{21} = AB - C > 0$ implies

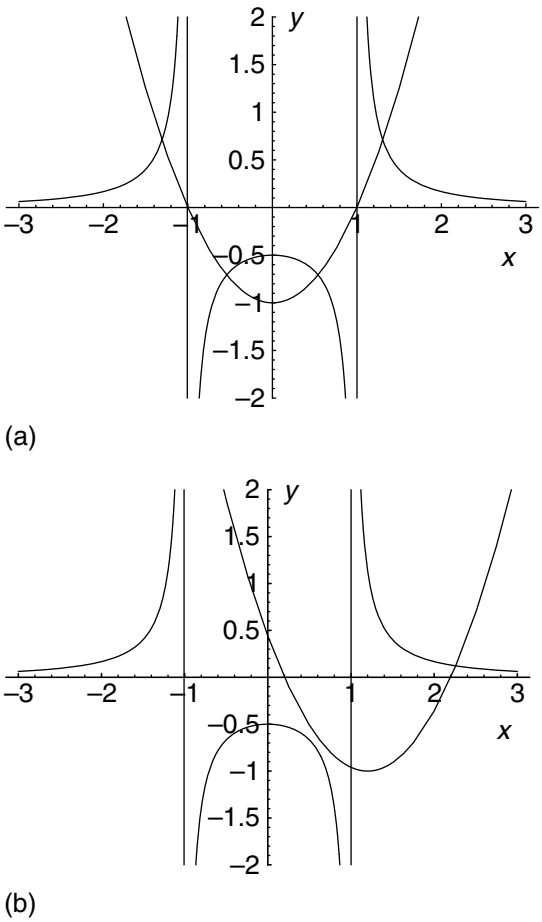

Figure 4. The functions $f_1(x)$ (parabola) and $f_2(x)$ (rational function, two vertical asymptotes) defined by equation (19) are depicted, versus x, for $A = B = -1$, $C = 0.5$, $x_2 = 0$ and (a) $x_1 = 0$ (equal group velocities); (a) $x_1 = 1.2$ (different group velocities). Recalling that the number of intersection points, i.e. 4 in (a) and 2 in (b), denote the number of real solutions of the dispersion relation (14), we see that a finite group velocity mismatch is capable of destabilizing a pair of (stable, separately) UH waves, which would otherwise be stable.

(for $B > 0$) that $A > C/B$; thus, the minimum of $f_1(x)$ lies always above the local maximum of $f_2(x)$. Thus, four points of intersection exist (cf figure 5(a)), for $x_1 = x_2$ and $A, B > 0$; this fact straightforward prescribes instability, as we saw, for $v_{g,1} = v_{g,2}$ and $M_{11}, M_{22} < 0$ (both UH waves individually unstable). Considering $v_{g,1} \neq v_{g,2}$ simply results in a horizontal shift between the two curves (cf figure 5(b)), which does not affect this qualitative result at all. Therefore, a pair of unstable UH waves remains unstable even in case of a finite difference in group velocity.

5. Modulated envelope UH soliton excitations

The system of coupled NLS equations (10) has been investigated in a number of theoretical works. It is known to be integrable for a specific choice of parameters, namely,

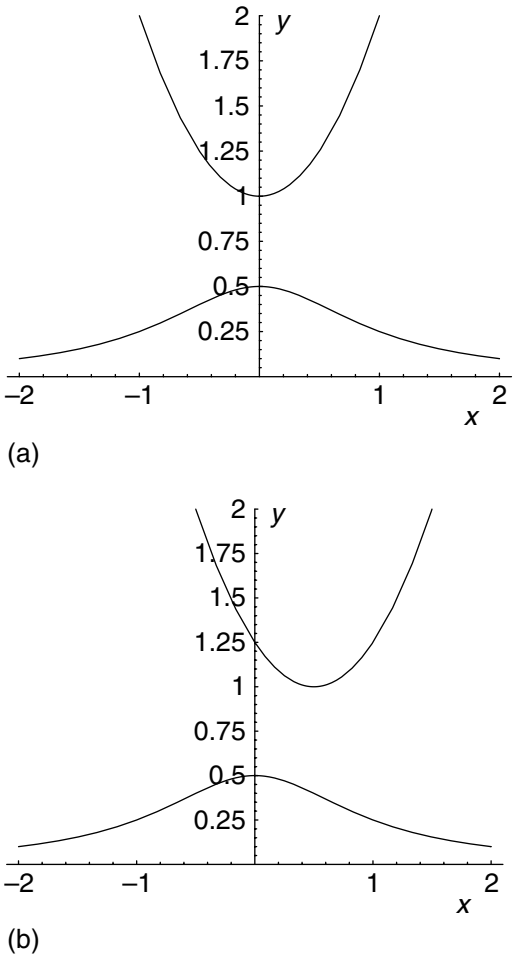

Figure 5. The functions $f_1(x)$ and $f_2(x)$ are depicted, for $A = B = +1$, $C = 0.5$, $x_2 = 0$ and (a) $x_1 = 0$ (equal group velocities); (a) $x_1 = 0.5$ (different group velocities). We see that a finite group velocity mismatch has no effect on a pair of (unstable, separately and together) UH waves.

if $Q_{12}/Q_{11} = Q_{21}/Q_{22} = 1$ [37, 38], where it is solved by the inverse scattering transform, as Manakov showed in his seminal work three decades ago [24]; this condition is indeed fulfilled here (equal group velocities need to be assumed though, as implied in Manakov's study). Various types of solutions have been shown to exist, including coupled bright envelope solitons (pulses) [24, 28, 39], bright-to-dark coupled envelope solitons [40]–[42], domain walls (obtained numerically) [43] and cnoidal waves [41, 44]. In the following, we shall briefly review some existing analytical results, which are of interest here, with respect to our coupled UH wave propagation problem.

5.1. Bright and dark single (uncoupled) envelope solitons

It may be instructive to consider the single wave (uncoupled) case, which is obtained, say, by setting $\mathcal{E}_2 = 0$ in equations (10). The (single) NLS equation is an integrable dynamical system [22] which admits, among others, localized solutions in the form of envelope solitons of the bright or dark (black/grey) type (for P_j positive or negative, respectively, in our case). Analytical

expressions for these solutions are found by inserting the trial function $\mathcal{E} = \mathcal{E}_0 \exp(\mathrm{i}\Theta)$ and then separating the real and imaginary parts in order to determine the (real) functions $\mathcal{E}_0(z, t)$ and $\Theta(z, t)$. Let us retain that this analytical ansatz amounts to a total electric field whose magnitude is essentially equal to $2\mathcal{E}_0 \cos(kz - \omega t + \Theta)$, where the localized field envelope amplitude $\mathcal{E}_0$ and the (small) phase shift Θ will be determined, case by case. Details on the derivation of their analytic form can be found in [35, 36], so only the final expressions are presented here.

A stationary soliton solution to the remaining (single) NLS equation may be sought in the form $\mathcal{E} = \exp(\mathrm{i}P\mu^2 t)\,\tilde{E}$ (an index 1 will be dropped in this paragraph, hence $\tilde{E} = \tilde{E}_1$, $P = P_1$ and $Q = Q_{11}$), where μ is a real constant and $\tilde{E}(z)$ is a real function to be determined. The general 'Galilean boosted' soliton solution of the (single) NLS is then given by

$$\mathcal{E} = \exp\left[\mathrm{i}(\tilde{k}z + \tilde{\omega}t + \Theta)\right]\tilde{E}(z - u_e t), \tag{20}$$

[35, 39], where u_e is the (arbitrary real) envelope velocity and $\tilde{k} = u_e/2P$, $\tilde{\omega} = P(\mu^2 - u_e^2/4P^2)$ and Θ are respectively small wavenumber, frequency and phase (constant) corrections (due to amplitude modulation), to be determined.

For $PQ > 0$, one finds the bright-type (pulse-shaped) envelope single soliton solution

$$\tilde{E}(z) = \pm\left(\frac{2P}{Q}\right)^{1/2} \mu\,\mathrm{sech}(\mu z), \tag{21}$$

[35, 39] where $\mathrm{sech}\,x = 1/\cosh x = 2[\exp x + \exp(-x)]^{-1}$ is the hyperbolic secant function. This excitation represents a localized envelope pulse confining the fast carrier oscillations. The phase shift Θ is a real (arbitrary) constant. Recalling equation (8), we see that a bright electric field envelope excitation is accompanied by a co-propagating negative density variation (a localized density void).

For $PQ < 0$, one finds the black-type soliton

$$\tilde{E}(z) = \pm\left|\frac{2P}{Q}\right|^{1/2} \mu|\tanh(\mu z)|, \tag{22}$$

where $\tanh x = \sinh x/\mathrm{sech}\,x = [\exp x - \exp(-x)]/[\exp x + \exp(-x)]$ is the hyperbolic tangent function. This excitation represents a propagating localized region of zero field value, i.e. a void inside an elsewhere finite oscillation amplitude region. The phase shift Θ is a real (arbitrary) constant.

For $PQ < 0$, one also obtains the grey-type soliton

$$\tilde{E}(z) = \pm\left|\frac{2P}{Q}\right|^{1/2} \frac{1}{d}\mu[1 - d^2\,\mathrm{sech}^2(\mu z)]^{1/2}, \tag{23}$$

representing a region of reduced (yet non-vanishing) electric field value (an envelope hole). Here, d is a real number ($|d| \leqslant 1$) which determines the localized electric field dip at the middle (for $s = z - u_e t = 0$). The black soliton (22) is recovered for $d = 1$. The phase shift Θ here is a complex (real) function of z and t [35] (omitted here for simplicity).

Once the electric field form is determined, the (co-propagating) density perturbation N is then readily given by expression (8), i.e. $N \sim -(|\mathcal{E}|^2 - |\mathcal{E}_\infty|^2)$. Interestingly, in all three of the above solutions, one obtains $N \sim -(2P\mu^2/Q)\mathrm{sech}^2(\mu z)$ (to see this, recall the identity

$\mathrm{sech}^2 x + \tanh^2 x = 1$). Therefore, a localized electron density depletion (negative pulse) is formed, being driven by the UH wave electric field envelopes.

Notice that the maximum amplitude $\mathcal{E}_{max} \sim (2P\mu^2/Q)^{1/2}$ of all these excitations is, in fact, inversely proportional to its spatial extension (width) $L = \mu^{-1}$, i.e. $\mathcal{E}_{max}L =$ constant (unlike KdV solitons, which formally satisfy $\mathcal{E}_{max}L^2 =$ constant; see [36] for a detailed discussion).

Summarizing, for a (frequency ratio) α below (above) 1/3, where P is positive (negative), the single UH wave is unstable (stable) and may propagate in the form of a bright (dark)-type modulated UH envelope wavepacket, i.e. a localized UH envelope hump against an elsewhere vanishing (constant) wave background; this electric field excitation is associated with a background density dip, i.e. a co-propagating region of density depletion.

5.2. Bright–bright coupled envelope solitons

Coupled soliton solutions to the set of equations (10) (for $v_{g,1} \approx v_{g,2}$) have been shown (see e.g. in [28, 39]) to exist in the form

$$\mathcal{E}_j = \exp\left[\mathrm{i}(\tilde{k}_j z + \tilde{\omega}_j t + \Theta_j)\right]\tilde{E}_j(z - u_e t), \tag{24}$$

(for $j = 1, 2$) [39], where $\tilde{k}_j = \xi_j$, $\tilde{\omega}_j = P_j(\mu_j^2 - \xi_j^2)$ and Θ_j are small wavenumber, frequency and phase corrections. Here $\mu_{1/2}$ and $\xi_{1/2}$ are real constants and $\tilde{E}_{1/2}(s)$ are real functions of $s = z - u_e t$, to be determined, while u_e is a (coupled) envelope velocity which satisfies $u_e = 2P_1\xi_1 = 2P_2\xi_2$ (hence $\xi_2 = \xi_1$, here).

The fundamental coupled bright-type (pulse-shaped) envelope solution takes the form $\tilde{E}_j(z) = a_j w(x; \mu^2)$ (for $j = 1, 2$), where w satisfies

$$w_{xx} - \mu^2 w + 2w^3 = 0.$$

The solution takes the form [28, 39]

$$\tilde{E}_j(z) = \pm a_j \mu_j \,\mathrm{sech}(\mu_j z), \tag{25}$$

which represents a pair of localized envelope pulses, confining the fast electric field oscillations in the two UH waves and co-propagating at the same speed u_e. The phase shift Θ is a real (arbitrary) constant. In general, the coefficients a_j satisfy the linear system

$$\frac{Q_{11}}{P_1}a_1^2 + \frac{Q_{12}}{P_1}a_2^2 = \frac{Q_{21}}{P_2}a_1^2 + \frac{Q_{22}}{P_2}a_2^2 = 2, \tag{26}$$

as shown in [28, 39]. Interestingly, the characteristic determinant $Q_{11}Q_{22} - Q_{12}Q_{21}$ vanishes here (since $Q_{ij} = Q$); still, these solutions will exist since $P_1 \approx P_2$ in our problem of interest. The solutions for a_j here satisfy $a_1^2 + a_2^2 = 2P/Q$. Now, from equation (8), we see that this bright–bright bi-envelope excitation is accompanied by a co-propagating positive density variation, i.e. a localized density dip in the formal form $N = \sum_j C_j \mathrm{sech}^2(\mu_j z)$; its form is determined by C_j, which are appropriate (positive, here) coefficients, i.e. functions of the parameters μ_1, μ_2 and of $k_1 \approx k_2$). The localized density variation N and the field envelopes $E_{1/2}$ propagate at the same velocity u_e and bear characteristics (relative magnitude, width) which depend on parameter values.

5.3. Bright–dark coupled envelope solitons

Searching for localized excitations characterized by vanishing boundary conditions for one of the waves, say $\mathcal{E}_1 \to 0$ as $z \to \pm\infty$, and finite ones for the other, i.e. $\mathcal{E}_2 \to a_2$ as $z \to \pm\infty$, one obtains a set of solutions in the form $\mathcal{E}_j = a_j \tilde{E}_j \exp[\mathrm{i}(\xi_j z - \tilde{\omega}_j t + \Theta_j)]$ (for $j = 1, 2$), with

$$\hat{E}_1 = \mu_1 \operatorname{sech}[\mu_1(z - u_e t)], \qquad \hat{E}_2 = \mu_2\{1 - d^2 \operatorname{sech}^2[\mu_2(z - u_e t)]\}^{1/2}, \quad (27)$$

where, same as above, the parameters μ_j and a_j need to be determined, along with a set of associated criteria for existence; details can be found in [28, 40, 42]. The parameters satisfy [40] $u_e = 2P_1\xi_1 = 2P_2\xi_2$ (i.e. $\xi_1 = \xi_2$ here), as in the bright–bright soliton pairs presented above. In general, no such solution occurs for $P_2 < 0 < P_1$ (this constraint is irrelevant here, since $P_1 = P_2$). We notice the real parameter $d^2 \leqslant 1$, which regulates the modulation depth of the grey (for $d^2 < 1$) or black (for $d^2 = 1$) excitation for $\hat{E}_2$; the black-type envelope $\hat{E}_2 = \mu_2 |\tanh[\mu_2(z - u_e t)]|$ is recovered for $d^2 = 1$.

In combination with equation (8) for the associated density variation, we notice that the latter takes the form $N = \sum_j C_j \operatorname{sech}^2(\mu_j z)$; however, the sign (either positive or negative) of N is not prescribed beforehand, since it is essentially determined by (the interplay between) μ_1 and μ_2 (via the coefficients C_j, which are to be determined); to see this, we notice that $|\mathcal{E}_2|^2 - |\mathcal{E}_{2,\infty}|^2 < 0 < |\mathcal{E}_1|^2 - |\mathcal{E}_{1,\infty}|^2$ in this case. Again, the localized density variation N and the field envelopes $E_{1/2}$ propagate at the same velocity u_e and bear characteristics (relative magnitude, width) which depend on parameter values.

6. Conclusions

We have presented an investigation of the behaviour of nonlinearly coupled UH waves, which propagate across the magnetic field, at different group velocities, near the UH resonance frequency. The nonlinear coupling between the two UH waves occurs due to quasi-stationary density perturbations that are driven by the ponderomotive forces of the two UH waves. Due to this nonlinear interaction, we have obtained a closed set of evolution equations for the modulated electric field amplitudes $\mathcal{E}_1$ and $\mathcal{E}_2$ of the UH waves, and the relative plasma density variation $N = n_1/n_0$. The evolution equations were then reduced to a pair of coupled NLS equations for the UH wave electric field envelopes.

The modulational stability analysis around a steady state of two coupled harmonic waves has shown that a pair of coupled UH waves may become unstable, if either (or both) is (are) individually (i.e. in the absence of one another) modulationally unstable. In the case where both waves are individually stable, mutual coupling may result in them being destabilized, in the presence of a finite group velocity mismatch.

Although our detailed analysis was explicitly limited to the region in the neighbourhood of the UH resonance, these qualitative results obtained are valid in a wider range of the UH carrier wavenumber values (i.e. for different $v_{g,j}$ and P_j; $j = 1, 2$), as one may readily verify via an extended graphic analysis along the lines proposed above. In order to obtain quantitatively rigorous analytical results (explicit stability criteria, perturbation wave number thresholds), an investigation should include the analysis of the full (fourth order polynomial) perturbation dispersion relation (14). This tedious task goes beyond the scope of this study; nevertheless, this generalized kind of study is under way, and should be reported soon.

In conclusion, we stress that the present investigation should help to understand the nonlinear propagation of two large amplitude colliding UH waves in magnetized plasmas, such as those in the Earth's magnetosphere and at the magnetopause. Specifically, future observations from the CLUSTER mission may reveal the signature of localized UH wave envelopes in association with density depression in the background plasma. Finally, laboratory experiments should also be conducted to verify the theoretical predictions that have been made herein.

Acknowledgments

This work was partially supported by the Deutsche Forschungsgemeinschaft (Bonn, Germany) through the Sonderforschungsbereich (SFB) 591, Universelles Verhalten Gleichgewichtsferner Plasmen: Heizung, Transport und Strukturbildung. IK is grateful to the Max-Planck-Institut für Extraterrestrische Physik (Garching, Germany) for the award of a fellowship (project: 'Complex Plasmas').

References

[1] Stix T 1992 *Waves in Plasmas* (New York: American Institute of Physics)
[2] Baumjohann W and Treumann R A 1996 *Basic Plasma Space Physics* (London: Imperial College Press)
[3] Décréau P M E, Fergeau P, Krasnosels'kikh V *et al* 2001 *Ann. Geophys.* **19** 1241
Szita S, Fazakerley A N, Carter P J *et al* 2001 *Ann. Geophys.* **19** 1711
[4] Hirshfield J L and Granatstein V L 1977 *IEEE Trans. Microwave Theory Tech.* **25** 522
[5] Tripathi V K and Sharma R R 1979 *Phys. Fluids* **22** 1799
Tripathi V K and Liu C S 1982 *Phys. Fluids* **25** 1388
[6] Kruer W L and Estabrook K 1977 *Phys. Fluids* **20** 1688
[7] Sugai H 1981 *Phys. Rev. Lett.* **47** 1899
[8] Porkolab M 1972 *Nucl. Fusion* **12** 329
[9] Kaufman A N and Stenflo L 1975 *Phys. Scr.* **11** 269
[10] Porkolab M and Goldman M V 1976 *Phys. Fluids* **19** 872
[11] Yu M Y and Shukla P K 1977 *Plasma Phys.* **19** 889
[12] Shukla P K 1977 *J. Plasma Phys.* **18** 249
[13] Turner J G and Boyd T J M 1979 *J. Plasma Phys.* **22** 121
[14] Shukla P K and Yu M Y 1982 *Phys. Rev. Lett.* **49** 696
[15] Sharma R P and Shukla P K 1983 *Phys. Fluids* **26** 87
[16] Rao N N 1988 *J. Plasma Phys.* **39** 385
[17] Shukla P K, Fedele R and de Angelis U 1985 *Phys. Rev.* A **31** 517
[18] Shukla P K, Eliasson B and Stenflo L 2003 *Phys. Rev.* E **68** 067401
[19] Eliasson B and Shukla P K 2003 *Phys. Plasmas* **10** 3539–44
[20] Hasegawa A 1975 *Plasma Instabilities and Nonlinear Effects* (Berlin: Springer)
[21] Remoissenet M 1994 *Waves Called Solitons* (Berlin: Springer)
[22] Sulem C and Sulem P L 1999 *The Nonlinear Schrödinger Equation* (Berlin: Springer)
[23] Ostrovskii L A 1967 *Sov. Phys.—JETP* **24** 797
[24] Manakov S V 1974 *Sov. Phys.—JETP* **38** 248
[25] Hasegawa A and Tappert F 1973 *Applied Phys. Lett.* **23** 142
[26] Agrawal G, Baldeck P L and Alfano R R 1989 *Phys. Rev.* A **39** 3406
[27] Das K P and Sihi S 1979 *J. Plasma Phys.* **21** 183
[28] Gupta M R, Som B K and Dasgupta B 1981 *J. Plasma Phys.* **25** 499
[29] Bilbault J M, Marquie P and Michaux B 1995 *Phys. Rev.* E **51** 817

[30] Kasamatsu K and Tsubota M 2004 *Phys. Rev. Lett.* **93** 100402
[31] Lazarides N and Tsironis G P 2005 *Phys. Rev.* E **71** 036614
[32] Kourakis I and Shukla P K 2005 *Phys. Rev.* E **71** in press
[33] Karpman V I and Washimi H 1976 *Sov. Phys.—JETP* **44** 528
[34] Karpman V I and Washimi H 1977 *J. Plasma Phys.* **18** 173
[35] Fedele R, Schamel H and Shukla P K 2002 *Phys. Scr.* T **98** 18
Fedele R and Schamel H 2002 *Eur. Phys. J.* B **27** 313
[36] Fedele R 2002 *Phys. Scr.* **65** 502
[37] Sahadevan R, Tamizhmani K M and Lakshmanan M 1986 *J. Phys. A: Math. Gen.* **19** 1783
[38] Radhakrishnan R, Sahadevan R and Lakshmanan M 1995 *Chaos, Solitons Fractals* **5** 2315
[39] Tan B and Boyd J P 2000 *Chaos, Solitons Fractals* T **11** 1113
[40] Vladimirov S V, Stenflo L and Yu M Y 1991 *Phys. Lett.* A **153** 144
[41] Inoue Y 1976 *J. Plasma Phys.* **16** 439
[42] Lisak M, Höök A and Anderson D 1990 *J. Opt. Soc. Am.* B **7** 810
[43] Haelterman M and Sheppard A P 1994 *Phys. Lett.* A **185** 265
[44] Hioe F T 1991 *Phys. Rev. Lett.* **82** 1152